DR CSABA JUHÁSZ (Orcid ID : 0000-0002-5067-5554)

Received Date : 31-Aug-2016

Revised Date : 17-Feb-2017

Accepted Date : 20-Feb-2017

Article type : Original Article

[original article: 3 figures, 2 tables; 1 online table]

Clinical and metabolic correlates of cerebral calcifications in Sturge–Weber syndrome

VINOD K PILLI[1]

MICHAEL E BEHEN[1]

JIANI HU[2]

YANG XUAN[2]

JAMES JANISSE[3]

HARRY T CHUGANI[1,4]

CSABA JUHÁSZ[1]

1 The Carman and Ann Adams Department of Pediatrics, Division of Pediatric Neurology, Children's Hospital of Michigan, Wayne State University, Detroit, MI; **2** Department of Radiology, Wayne State University, Detroit, MI; **3** Department of Family Medicine and Public

Health Sciences, Wayne State University, Detroit, MI; **4** Division of Neurology, Nemours/Alfred I DuPont Hospital for Children, Wilmington, DE, USA.

Correspondence to Csaba Juhász at Wayne State University School of Medicine, PET Center and Translational Imaging Laboratory, Children's Hospital of Michigan, 3901 Beaubien St., Detroit, MI 48201, USA. E-mail: juhasz@pet.wayne.edu

PUBLICATION DATA

Accepted for publication 20th February 2017.

Published online 00 Month 2017.

ABBREVIATIONS

FDG-PET 2-deoxy-2-[^{18}F]fluoro-D-glucose positron emission tomography

FDR False discovery rate

SWI Susceptibility weighted imaging

SWS Sturge–Weber syndrome

[abstract]

AIM To evaluate clinical and metabolic correlates of cerebral calcifications in children with Sturge–Weber syndrome (SWS).

METHOD Fifteen children (11 female, 4 male; age range 7mo–9y 0mo, mean 4y 1mo) with unilateral SWS underwent baseline and follow-up magnetic resonance imaging (MRI) with susceptibility weighted imaging (SWI), glucose metabolism positron emission tomography (PET), and neurocognitive assessment (mean follow-up 1y 7mo). Calcified brain volumes measured on SWI were correlated with areas of abnormal glucose metabolism, seizure variables, and cognitive function (intelligence quotient [IQ]).

RESULTS Ten children had brain calcification at baseline and 11 at follow-up. Mean calcified brain volume increased from 1.67 to 2.7cm^3 (p=0.003) in these children; the rate of interval calcified volume increase was associated with early onset of epilepsy (Spearman's rho [r_s]=–0.63, p=0.036). Calcified brain regions showed a variable degree of glucose hypometabolism with the metabolic abnormalities often extending to non-calcified cerebral lobes. Larger calcified

brain volumes at baseline were associated with longer duration of epilepsy (r_s=0.69, p=0.004) and lower outcome IQ (r_s=–0.53, p=0.042).

INTERPRETATION Brain calcifications are common and progress faster in SWS children with early epilepsy onset, and are associated with a variable degree of hypometabolism, which is typically more extensive than the calcified area. Higher calcified brain volumes may indicate a risk for poorer neurocognitive outcome.

[first page footer]

DOI:

[Left page footer]

Developmental Medicine & Child Neurology 2017, 59: 000−000

[Right page footer]

Progressive Cerebral Calcifications in Sturge–Weber Syndrome *Vinod K Pilli et al*.

What this paper adds

- Brain calcifications progress faster in children with Sturge–Weber syndrome (SWS) and early-onset epilepsy.
- Hypometabolism often extends beyond calcified brain regions.
- Calcified brain volume may be an imaging biomarker for cognitive outcome in SWS.

[main text]

Sturge–Weber syndrome (SWS) is a sporadic neurocutaneous syndrome with a facial port-wine birthmark and ipsilateral leptomeningeal vascular malformation in the brain. The most common neurological symptoms include seizures, hemiparesis, and visual field deficit. The intracranial pathology in SWS is most commonly unilateral, and about 50% of children with SWS have impaired cognitive development.[1] A significant proportion of these children has progressive cognitive decline during the early course of the disease, but the individual course is highly

variable.[2] A recent, longitudinal study identified a number of potential clinical and electroencephalography (EEG) predictors of neurocognitive outcome.[2]

Magnetic resonance imaging (MRI) is most often used to detect intracranial involvement in SWS; conventional MRI can demonstrate abnormal contrast-enhancing leptomeningeal vessels, enlarged choroid plexus, as well as cortical and white matter atrophy.[1,3] Cerebral calcifications are also common and can be detected by both computed tomography and MRI.[4,5] Although progressive calcification in SWS has been demonstrated by computed tomography,[4] the timing, rate, and clinical correlates of such progression remain to be determined.

Susceptibility weighted imaging (SWI) is an MRI technique sensitive to small changes in local magnetic susceptibility in the brain tissue and is used to enhance the native contrast of different tissue types.[6] When compared with other MRI techniques, SWI has been shown to have superior sensitivity to detect calcifications and small venous abnormalities in children with SWS.[7,8] In our previous, cross-sectional study, severe calcification on SWI was associated with decreased perfusion in the affected SWS brain regions.[5] Calcification has also been implicated in epileptogenesis in brain lesions with various etiologies, including neurocysticercosis and SWS.[9,10]

The main goal of the present study was to evaluate cerebral calcifications quantitatively in children with unilateral SWS. We tested whether SWI is able to detect progressive calcification during the early disease course, and we also assessed the metabolic correlates of calcified brain regions using 2-deoxy-2-[^{18}F]fluoro-D-glucose positron emission tomography (FDG-PET). Finally, we evaluated whether the volume of calcified brain tissue could be an imaging marker for neurocognitive functioning.

METHOD

Participants

Fifteen children (11 female, 4 male; age range 7mo–9y 0mo, mean 4y 1mo) with unilateral SWS were selected for the study (Table SI, online supporting information) from a pool of children enrolled in a prospective, longitudinal neuroimaging study of children with SWS at the Children's Hospital of Michigan between 2004 and 2014. All patients met the following inclusion criteria: (1) MRI evidence of unilateral SWS brain involvement; (2) availability of MRI including a good quality SWI sequence both at baseline and at follow-up (mean follow-up

1y 8mo, range 1–3y); (3) availability of interictal FDG-PET; and (4) detailed neurocognitive assessment. No apparent MRI abnormalities were seen in the contralateral hemisphere in any of the patients. The study was approved by the institutional review board at Wayne State University and written informed consent of the parent or legal guardian was obtained.

Neuropsychological evaluation

All children underwent a comprehensive neuropsychological assessment within 1 day of the follow-up MRI studies, as described previously. Children from 2 years 6 months to 7 years 3 months of age were administered the Wechsler Pre-school and Primary Scale of Intelligence-III (WPPSI-III), and children older than 7 years 3 months, the Wechsler Intelligence Scales for Children-III (WISC-III). Both Wechsler scales provide indices of global cognitive functioning as expressed by an intelligence quotient (IQ); for simplicity, we used the full scale IQ in this study, because our previous study in children with SWS found that performance and verbal IQs show similar correlations with imaging and other clinical variables but did not significantly differ by laterality of the brain lesion.[11]

MRI acquisitions

MRI studies were performed on a Siemens Sonata 1.5 T or a MAGNETOM Verio 3T scanner (Siemens Medical Solutions, Erlangen, Germany) located at the Harper Hospital, Wayne State University. Repeated images were acquired on the same scanner in all but one patient. On both scanners, MRI acquisition included an axial T1 3-dimensional magnetization prepared rapid gradient echo (1mm slice thickness), an axial fluid attenuated inversion recovery, an axial T2-weighted turbo spin-echo acquisition, SWI, followed by post-contrast dynamic magnetic resonance perfusion-weighted imaging and axial magnetization prepared rapid gradient echo. SWI parameters were: (1) 1.5 T scanner: SWI acquisition was performed with a 3-dimensional fully balanced gradient-echo sequence with flip angle 20°; echo-planar imaging factor 5; acquisition matrix 512×256×48; field of view 256×256×96 mm^3; voxel size 0.5×0.5×2 mm^3; TR/TE 89/40ms; bandwidth 160Hz/pixel.[8] (2) 3 T scanner: field of view 224×168×128 mm; base resolution 448; voxel size 0.5×0.5×1 mm^3; partition number 96; TR/TE 30/18ms; bandwidth 90~120Hz/pixel, 2× accelerated GRAPPA paralleling imaging with 24 reference lines, and 6/8 partial Fourier along phase encoding.

FDG-PET acquisition

The details of FDG-PET acquisition in SWS have been described previously.[12] In brief, PET scans were acquired within 24 hours of MRI acquisitions using an EXACT/HR PET scanner (CTI/Siemens, Hoffman Estates, IL, USA) or a GE Discovery STE PET/computed tomography scanner (GE Medical Systems, Milwaukee, WI, USA). Both scanners have a 15cm field of view and generate 47 image planes with a slice thickness of 3mm. The reconstructed image resolution was 5.5±0.35mm at full width at half-maximum in-plane and 6.0±0.49mm at full width at half-maximum in the axial direction. Scalp EEG was monitored in all children during the tracer uptake period and showed that all studies were interictal. Forty minutes after 0.143mCi/kg FDG injection, a static 20-min emission scan was acquired. Calculated attenuation correction was applied to the images using automated threshold fits to the sinogram data.

During both MRI and PET acquisition, children were sedated with pentobarbital (1.5–3 mcg/kg) and midazolam (0.1–0.2 mcg/kg); or by midazolam (0.1–0.2 mcg/kg) followed by dexmedetomidine (1–2 mcg/kg), titrated slowly to achieve mild to moderate sedation. In some cases, fentanyl (1 mcg/kg) was used as necessary in conjunction with either pentobarbital or midazolam. All sedated children were continuously monitored by a pediatric nurse specialized in sedation, and physiological parameters (heart rate, pulse oximetry) were monitored throughout the study.

Image analysis

All SWI images were processed offline using SPIN (Signal Processing in NMR), an in-house software. These post-processed SWI images were used for further evaluation.[6] Areas of calcification were visualized as low-intensity (black) areas on the SWI phase and magnitude images.[8] The SWI-detected calcified lesions were visualized and verified on corresponding planes of computed tomography scans where available, for comparison (Fig. 1).

Calcification volume was measured by regions of interest placed on filtered SWI phase images manually in each plane including all voxels consistent with calcification, using AMIDE software (version 1.0.4; http://amide.sourceforge.net). This analysis was performed by a single investigator (VKP) who was blinded to the clinical data of the subjects. The total volume (mm^3) of calcified brain tissue in the affected hemisphere was calculated both at baseline and follow-up.

Finally, to evaluate glucose metabolic abnormalities in areas with and without calcification, SWI images were co-registered with corresponding FDG-PET images using Vinci software (VINCI 3.80.0, Max Planck Institute, Cologne, Germany). Lobar location(s) and severity (mild/moderate/severe) of hypo- or hypermetabolism (compared with the homotopic cortex in the contralateral, unaffected hemisphere) were noted for each PET scan by the consensus of two of the investigators.

Seizure frequency and EEG severity scores

Seizure frequency and EEG severity scores were determined as described previously.[2] In brief, a seizure frequency score was assigned to each patient based on clinical seizures occurring during the 1-year period prior to the imaging study. The scores were determined as follows: 0, no seizures in the previous year; 1, one to 11 seizures per year; 2, one to four seizures per month; 3, more than four seizures per month. As most patients presented with focal motor seizures, seizure type was not separately assessed. EEG severity was scored on a scale of 0 to 3, where: 0, normal EEG; 1, focal voltage asymmetry (with or without slowing) without epileptiform discharges; 2, sporadic, unilateral epileptiform activity (≤10/min); 3, frequent epileptiform activity (>10/min). The frequency of epileptiform discharges was based on the area/side showing the highest spike frequency.

Statistical analysis

The total hemispheric volume of calcified brain tissue on SWI images was correlated with clinical variables (age at epilepsy onset, epilepsy duration, seizure frequency score, EEG score, and IQ) using Spearman's rank correlation. Monthly rate of change in calcified volume was also calculated from baseline and follow-up volume differences, divided by the time interval between the two scans (in months; only in those patients who showed calcification at follow-up) and correlated with age at seizure onset and duration of epilepsy. To control for inflated alpha in the testing of multiple correlations, a false discovery rate (FDR) procedure was employed.[13] Unadjusted and FDR adjusted *p*-values are presented. Differences between baseline and follow-up calcified volume were assessed by the Wilcoxon signed-rank test. All statistical analyses were performed using SPSS statistics for Windows (Release 23.0; SPSS, Chicago, IL, USA), and a *p*-value less than 0.05 was considered to be significant.

RESULTS

Clinical correlates of baseline calcification

Ten patients (67%) had cerebral calcification detected in the affected hemisphere on baseline SWI (see lobar locations and measured volumes in Table I); the mean volume of these calcified regions was 1.69cm^3 (standard deviation [SD] 1.95cm^3). Location and extent of the calcified areas matched well with calcification detected by computed tomography (see example on Fig. 1). Larger calcified brain volume on SWI at baseline was associated with longer duration of epilepsy at baseline (Spearman's rho [r_s]=0.69, p=0.004, unadjusted), younger age at seizure onset (r_s=–0.68, p=0.008, unadjusted), and lower IQ measured at follow-up (r_s=–0.53, p=0.042, unadjusted); this latter correlation only showed a trend after FDR adjustment (p=0.070) (Table II). No correlation was found between baseline calcified brain volume and seizure frequency scores or EEG severity scores.

Longitudinal changes of calcified brain volume

Eleven of the 15 patients had calcification detected on follow-up SWI, including one who had no visible calcification at baseline and a small area of new calcification 2 years later (patient #5 in Table SI). In these 11 children, mean calcified brain volume increased to 2.47cm^3 (SD 2.23cm^3) at follow-up (p=0.003); the monthly rate of interval calcification volume increase varied widely across patients (2–167mm^3 per month; mean +56 mm^3 per month) and was more robust in those with younger age at epilepsy onset (r_s=–0.63, p=0.036, unadjusted) (Table II). Larger calcified brain volume at follow-up was associated with longer duration of epilepsy and lower outcome IQ (Table II). In contrast, calcified brain volume at follow-up did not correlate with seizure frequency scores. Patient #3 had a third follow-up MRI with SWI 10 years after the second scan and demonstrated the continuing progression of calcification (Fig. 2).

FDG-PET correlates of calcified areas

All 15 patients showed abnormal glucose metabolism in the affected hemisphere, including the four children with no calcification on SWI (Table SI; Fig. 3). Altogether, all 28 calcified lobes in the affected hemispheres showed some level of hypometabolism on PET (varying from mild to severe) (Table SI, Fig. 3). In addition, abnormal glucose metabolism (mostly mild/moderate

hypometabolism) extended beyond the calcified lobe in 6 out of 11 patients with calcifications (details in Table SI).

DISCUSSION

To our knowledge, this is the first study to document the progression of SWS-associated brain calcification using a quantitative MRI approach. Our findings demonstrate a high inter-individual variability of the rate of progressive calcium build-up in affected brain regions, and show that children with early onset seizures are at high risk for greater calcification volumes and faster progression. In addition, our combined MRI/PET analysis demonstrates that while calcified brain regions occupy a relatively limited brain volume, they commonly show metabolic abnormalities extending into non-calcified regions. Importantly, the association between calcified brain volume and cognitive function indicates that SWI-detected calcifications may serve as an objective imaging marker for cognitive outcome during the early disease course.

Our group has previously reported the relation between cortical glucose hypometabolism and cognitive functions in SWS children in a cross-sectional study.[11] In that cohort, the extent of overall hypometabolism showed a negative correlation with IQ, similar to our current findings with the calcified brain volume. Our MRI/PET comparative results in the present study, showing that calcification is often associated with mild or moderate hypometabolism that often extends to adjacent lobes, is consistent with the notion that hypometabolic (but still functional) cortex may exert a "nociferous" effect on the rest of the brain – a concept originally introduced by Penfield[14] and supported by our previous SWS PET data.[11,15] Partly preserved metabolism in calcified regions can also explain the observation that such regions can retain language and motor functions,[16] presumably because of remaining functional neuronal tissue. On the other hand, our previous study[11] also demonstrated a non-linear ('U-shaped') curve between IQ and hemispheric extent of severely hypometabolic cortex, where function began to increase above 60% extent of severe hypometabolism in the affected hemisphere. We suggested that the bottom of the 'U' indicated the point at which intrahemispheric reorganization switched to interhemispheric reorganization, a notion that has received some support in the work of others using a different model of brain injury.[17,18] Taken together, our results demonstrate that while calcified regions can sustain some degree of metabolic activity, these areas typically are compromised

functionally, with mild/moderate hypometabolism often extending to larger areas thus leading to brain dysfunction and neurocognitive impairment.

Calcium deposits in SWS can contribute to brain damage through various mechanisms. Calcification is typically perivascular, with deposits forming a sleeve encrusting small vessels.[19] Calcium concretions also may be observed in the brain parenchyma along with gliosis in adjacent regions with focal necrosis and dystrophic calcification. Therefore, calcium deposits can be surrounded by areas of neuronal damage and gliosis that may contribute to hypometabolism observed on PET. In addition, the impact of calcified areas on brain function may be enhanced by their location in deep cortex and subcortical white matter, where they are positioned to disrupt cortical connections. In our previous study, severely calcified cortex was also associated with low perfusion in the subcortical white matter.[5] Hypometabolism in non-calcified regions may also be caused by mechanisms not related to calcium deposits. For example, a recent study demonstrated that microscopic (type I or type IIa) cortical dysplasia was common in SWS surgical specimens even if MRI could not identify cortical developmental abnormalities.[20] Such mild dysplastic areas may be hypometabolic on PET even in MRI-negative regions and contribute to hypometabolism in the affected hemisphere.

Cortical calcium deposits are also highly epileptogenic: accumulation of calcium phosphate crystals can raise ionized calcium concentrations in the brain parenchyma (adjacent to neurons), thus leading to increased neuronal excitability, focal seizures, and neuronal dysfunction.[21–24] Thus, calcium deposits in the SWS brain have the potential for an impact on both epilepsy and neurocognitive dysfunction. This effect may be diminished in areas which progress to the point of severe atrophy with no or minimal metabolism. Alternatively, such calcified areas may be stabilized by pharmacologic treatment. A beneficial clinical effect on symptomatic brain calcifications has been reported with the use of the calcium chelator etidronate, a common drug to treat diseases of bone and calcium metabolism.[25] Although anecdotal, these pilot results may justify clinical trials with similar drugs to alleviate SWS-associated neurological symptoms such as seizures and headaches in patients with massive cerebral calcifications.

MRI-detected calcified brain volume adds to the list of clinical and imaging parameters found to have prognostic value in our recent longitudinal study of children with SWS.[2] In that study, early seizure onset, high seizure frequency, early scalp EEG abnormalities, and frontal

lobe involvement on MRI were associated with poor IQ at follow-up. The current study adds calcified brain volume as a potential imaging marker of cognitive outcome. Future studies with a larger patient group should determine if calcifications are independent prognostic imaging markers of neurocognitive outcome in SWS.

Study limitations

Despite the prospective, longitudinal design and novel findings, our study has some inherent limitations. The study population was relatively small because of the rarity of SWS. To address the potential issue of type I statistical error, we calculated FDR-adjusted *p*-values, some of which showed a trend but were not significant. While these trends are of interest, we acknowledge that a final, definitive conclusion could only be made with a larger patient population. This is a common issue in rare conditions and warrants the design of multicenter studies. The age of the patients varied widely; however, all 15 patients were tested by WPPSI-III or WISC-III at follow-up and, therefore, outcome IQs are comparable across the entire group. The MRI studies were performed on two different scanners, but the same scanner was used in all but one individual case. In addition, none of the clinical or imaging variables differed significantly between the two scanners (data not shown); therefore, variations in the MR scanner are unlikely to have substantially affected the overall results. Finally, calcified brain volumes on SWI were delineated manually. Although not operator-independent, this procedure was performed by a single investigator who was blinded to the clinical data. Therefore, while slight inaccuracies in the absolute volumes may have occurred, the overall result of the consistently progressive progression of calcified volume and associations with clinical variables should be valid.

In conclusion, our data demonstrate that cerebral calcification is common and progressive in young children with SWS, progressing particularly rapidly in those with early epilepsy onset. Despite its modest overall volume, calcified brain is often associated with larger areas of hypometabolism detected by PET. Calcified brain volume may be used as an objective MRI biomarker to assist the clinical evaluation and prognostication of children with unilateral SWS.

ACKNOWLEDGEMENTS

We thank Cynthia Burnett and Cathie Germain for assisting patient recruitment and scheduling; Jane Cornett and Anne Deboard for performing sedation. We are also grateful to the Sturge–

Weber Foundation and the families who participated in these studies. This study was partially funded by a grant from the National Institutes of Health (R01 NS041922). HTC changed affiliation during the writing of this article, from Wayne State University to Nemours/Alfred I DuPont hospital. The authors have stated that they had no interests which might be perceived as posing a conflict or bias.

SUPPORTING INFORMATION

The following additional material may be found online:

Table SI: Clinical data of the 15 children with Sturge–Weber syndrome.

REFERENCES

1. Lo W, Marchuk DA, Ball KL, et al. Updates and future horizons on the understanding, diagnosis, and treatment of Sturge–Weber syndrome brain involvement. *Dev Med Child Neurol* 2012; **54**: 214–23.

2. Bosnyak E, Behen ME, Guy WC, et al. Predictors of cognitive functions in children with Sturge–Weber syndrome: a longitudinal study. *Pediatr Neurol* 2016; **61**: 38–45.

3. Juhász C, Chugani H. Imaging brain structure and function in Sturge–Weber syndrome. In: Bodensteiner JB, Roach ES, editors. Sturge–Weber syndrome. Mt Freedom, NJ: The Sturge–Weber Foundation, 2010: 109–48.

4. Pascual-Castroviejo I, Diaz-Gonzalez C, Garcia-Melian RM, et al. Sturge–Weber syndrome: study of 40 patients. *Pediatr Neurol* 1993; **9**: 283–8.

5. Wu J, Tarabishy B, Hu J, et al. Cortical calcification in Sturge–Weber Syndrome on MRI–SWI: relation to brain perfusion status and seizure severity. *J Magn Reson Imaging* 2011; **34**: 791–8.

6. Haacke EM, Xu Y, Cheng YC, Reichenbach JR. Susceptibility weighted imaging (SWI). *Magnetic Reson Med* 2004; **52**: 612–8.

7. Juhasz C, Haacke EM, Hu J, et al. Multimodality imaging of cortical and white matter abnormalities in Sturge–Weber syndrome. *AJNR Am J Neuroradiol* 2007; **28**: 900–6.

8. Hu J, Yu Y, Juhasz C, et al. MR susceptibility weighted imaging (SWI) complements conventional contrast enhanced T1 weighted MRI in characterizing brain abnormalities of Sturge–Weber Syndrome. *J Magn Reson Imaging* 2008; **28**: 300–7.

9. Nash TE, Mahanty S, Loeb JA, et al. Neurocysticercosis: A natural human model of epileptogenesis. *Epilepsia* 2015; **56**: 177–83.

10. Pinto A, Sahin M, Pearl PL. Epileptogenesis in neurocutaneous disorders with focus in Sturge Weber syndrome. *F1000Res* 2016; **5**: F1000 Faculty Rev–370.

11. Behen ME, Juhasz C, Wolfe-Christensen C, et al. Brain damage and IQ in unilateral Sturge–Weber syndrome: support for a 'fresh start' hypothesis. *Epilepsy Behav* 2011; **22**: 352–7.

12. Alkonyi B, Chugani HT, Juhasz C. Transient focal cortical increase of interictal glucose metabolism in Sturge–Weber syndrome: implications for epileptogenesis. *Epilepsia* 2011; **52**: 1265–72.

13. Benjamini Y, Hochberg Y. Controlling the false discovery rate: A practical and powerful approach to multiple testing. *J Royal Stat Soc B* 1995; **57**: 289–300.

14. Penfield W. Ablation of abnormal cortex in cerebral palsy. *J Neurol Neurosurg Psychiatry* 1952; **15**: 73–8.

15. Lee JS, Asano E, Muzik O, et al. Sturge–Weber syndrome: correlation between clinical course and FDG PET findings. *Neurology* 2001; **57**: 189–95.

16. Muller RA, Chugani HT, Muzik O, et al. Language and motor functions activate calcified hemisphere in patients with Sturge–Weber syndrome: a positron emission tomography study. *J Child Neurol* 1997; **12**: 431–7.

17. Irle E. An analysis of the correlation of lesion size, localization and behavioral effects in 283 published studies of cortical and subcortical lesions in old-world monkeys. *Brain Res Brain Res Rev* 1990; **15**: 181–213.

18. Bates E. Origins of language disorders: A comparative approach. *Dev Neuropsychol* 1997; **13**: 447–76.

19. McCartney E, Squier W. Patterns and pathways of calcification in the developing brain. *Dev Med Child Neurol* 2014; **56**: 1009–15.

20. Pinto AL, Chen L, Friedman R, et al. Sturge–Weber syndrome: brain magnetic resonance imaging and neuropathology findings. *Pediatr Neurol* 2016; **58**: 25–30.

21. Smeyers-Verbeke J, Michotte Y, Pelsmaeckers J, et al. The chemical composition of idiopathic nonarteriosclerotic cerebral calcifications. *Neurology* 1975; **25**: 48–57.

22. Dichter MA. Basic mechanisms of epilepsy: targets for therapeutic intervention. *Epilepsia* 1997; **38 Suppl 9**: S2–6.

23. Stefani A, Spadoni F, Bernardi G. Voltage-activated calcium channels: targets of antiepileptic drug therapy? *Epilepsia* 1997; **38**: 959–65.

24. DeLorenzo RJ, Pal S, Sombati S. Prolonged activation of the N-methyl-D-aspartate receptor-Ca2+ transduction pathway causes spontaneous recurrent epileptiform discharges in hippocampal neurons in culture. *Proc Natl Acad Sci USA* 1998; **95**: 14482–7.

25. Loeb JA, Sohrab SA, Huq M, Fuerst DR. Brain calcifications induce neurological dysfunction that can be reversed by a bone drug. *J Neurol Sci* 2006; **243**: 77–81.

Table I: Imaging findings of the 15 children with Sturge–Weber syndrome

Pt. no.	LMA lobe(s) on MRI	Calcification			FDG-PET areas of hypometabolism	
		Lobes involved	Volume at baseline (mm^3)	Volume at follow-up (mm^3)	Baseline	Follow-up
1	R FTPO	TPO	1112	3463	mild *F*TP[a]	mod/sev TPO; mild *F*
2	R FTPO	F	362	578	mild F*P*[a]	mod/sev *TPO*; mild/mod F
3	R TPO	TP	75	1162	mild TP*O*	mild TP*O*
4	L TPO	none	0	0	mild *O*	mild *O*
5	L P	P	0	75	mild *T*P	mild *T*P
6	L FTPO	FTPO	822	2826	mod/sev F; sev TPO	mod/sev F; sev TPO
7	L TPO	TPO	861	1111	n/a	mod/sev *F*; sev TPO
8	R P	P	194	244	mild P	mild P
9	L FTPO	TPO	5720	6876	mild *F*TO; mod P	mild *F*; mod TPO
10	R FTPO	FTPO	1893	2504	mod/sev FTP; mild O	mod/sev FTP; mild O
11	R TO	none	0	0	mild *TPO*	mild *TPO*
12	L FTPO	TPO	1175	2471	mild TP; mod O	mod TO; mild P
13	L FP	none	0	0	mild/mod *TPO*	mild/mod *TPO*
14	L FTPO	FTPO	4728	5839	mod TPO	mod TPO; mild F
15	R TPO	None	0	0	mild/mod *TPO*	mod/sev *TPO*

Lobes in *italic* indicate non-calcified lobes with glucose metabolic abnormalities. [a]Lobe showed hypermetabolism on FDG-PET. Mod, moderate; sev, severe (hypometabolism); SWS, Sturge–Weber syndrome; LMA, leptomeningeal angiomatosis; MRI, magnetic

resonance imaging; FDG-PET, 2-deoxy-2-[^{18}F]fluoro-D-glucose positron emission tomography; R, right; F, frontal; T, temporal; P, parietal; O, occipital; L, left.

Table II: Spearman's rank correlations between calcification volumes and clinical variables

MRI variable (calcification volume)	Clinical variable	Spearman's rho	Unadjusted *p*	FDR-adjusted *p*
Baseline	Epilepsy duration 1 (*n*=15)	0.69	0.004	0.039
	Age at onset (*n*=14)	-0.68	0.008	0.039
	IQ (*n*=15)	-0.53	0.042	0.070
	EEG severity (*n*=15)	0.41	0.127	0.182
	Seizure frequency 1 (*n*=14)	0.21	0.462	0.577
Follow-up	Epilepsy duration 2 (*n*=15)	0.56	0.028	0.070
	IQ (*n*=15)	-0.61	0.016	0.053
	Seizure frequency 2 (*n*=15)	0.06	0.842	0.842
Monthly rate of volume change	Age at onset (*n*=11)	-0.63	0.036	0.070
	Duration of epilepsy (*n*=11)	0.14	0.679	0.754

Age at onset was not included in one child who never had seizures. Monthly rate of calcification volume change was only calculated for 11 children who showed calcification during follow-up. MRI, magnetic resonance imaging; FDR, false discovery rate; IQ, intelligence quotient; EEG, electroencephalogram.

Figure 1: Demonstration of brain calcification on computed tomography (CT) and susceptibility weighted imaging (SWI; both magnitude and phase images are shown). The images are from a 4-year-old female (patient #10) with extensive right hemispheric involvement. Both computed tomography and SWI detected calcification in the lateral frontal and temporo-parieto-occipital cortex.

Figure 2: Enlarged MRI (susceptibility weighted imaging, SWI) magnitude and phase images at baseline and follow-up in a 21-month-old male (patient #3) with right posterior hemispheric involvement and minimal calcification at baseline. SWI showed progressive calcification in the right parietal and temporal lobe (arrows), with calcified brain volume increasing on follow-up images at age 3 years; this patient also had a second follow-up MRI at age 13 years, demonstrating further progression in the calcified area.

Figure 3: Co-registered axial susceptibility weighted imaging (SWI) phase and 2-deoxy-2-[^{18}F]fluoro-D-glucose positron emission tomography (FDG-PET) image planes from three Sturge–Weber syndrome (SWS) patients. (A) Patient #9 had left parietal (along with temporo-occipital, not shown) calcification (white arrows). The left parietal cortex showed moderate hypometabolism on PET (green area, red arrow), while the non-calcified frontal cortex showed mild hypometabolism (red arrowhead) compared with the contralateral unaffected side. (B) Left temporo-occipital and also frontal calcifications (white arrows) in patient #14. While the left temporo-occipital cortex (along with the left thalamus) showed severe hypometabolism (blue area, red arrow), the calcified frontal cortex showed largely preserved glucose metabolism, except for a mild decrease in the posterior frontal region (red arrowhead). (C) Patient #15 had no evidence of calcification on SWI, while PET showed moderate (green area) to severe (blue area) hypometabolism (red arrows) in the right temporo-occipital (and also parietal, not shown) cortex.

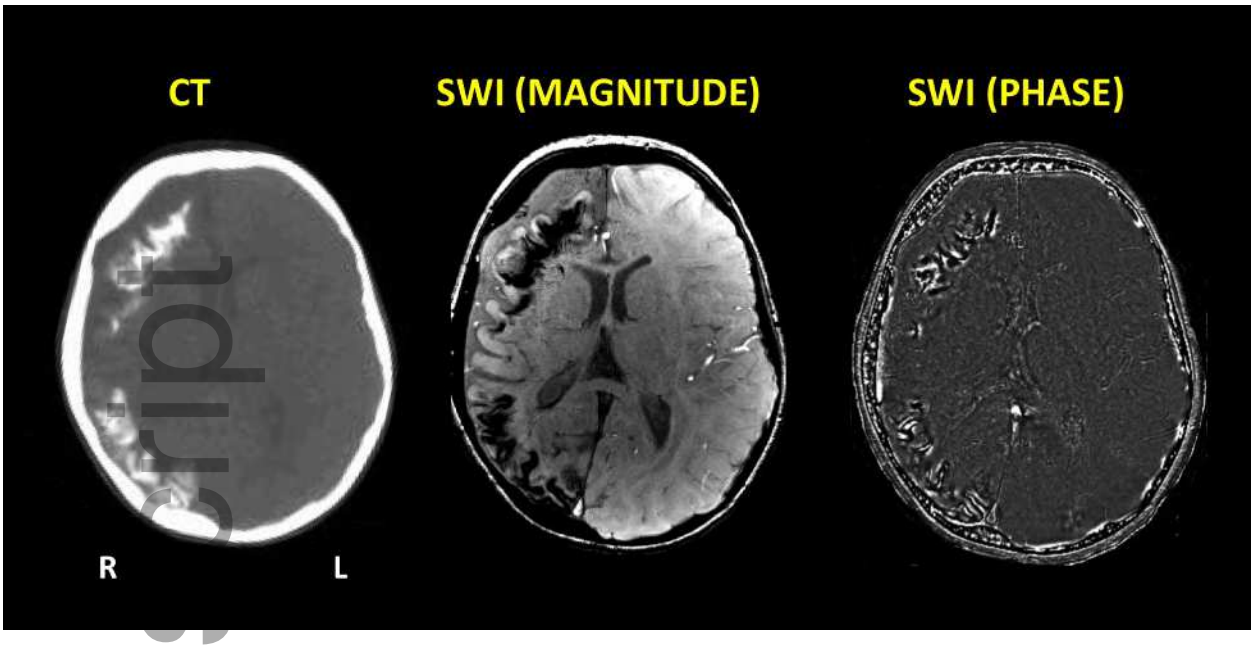

dmcn_13433_f1.jpg

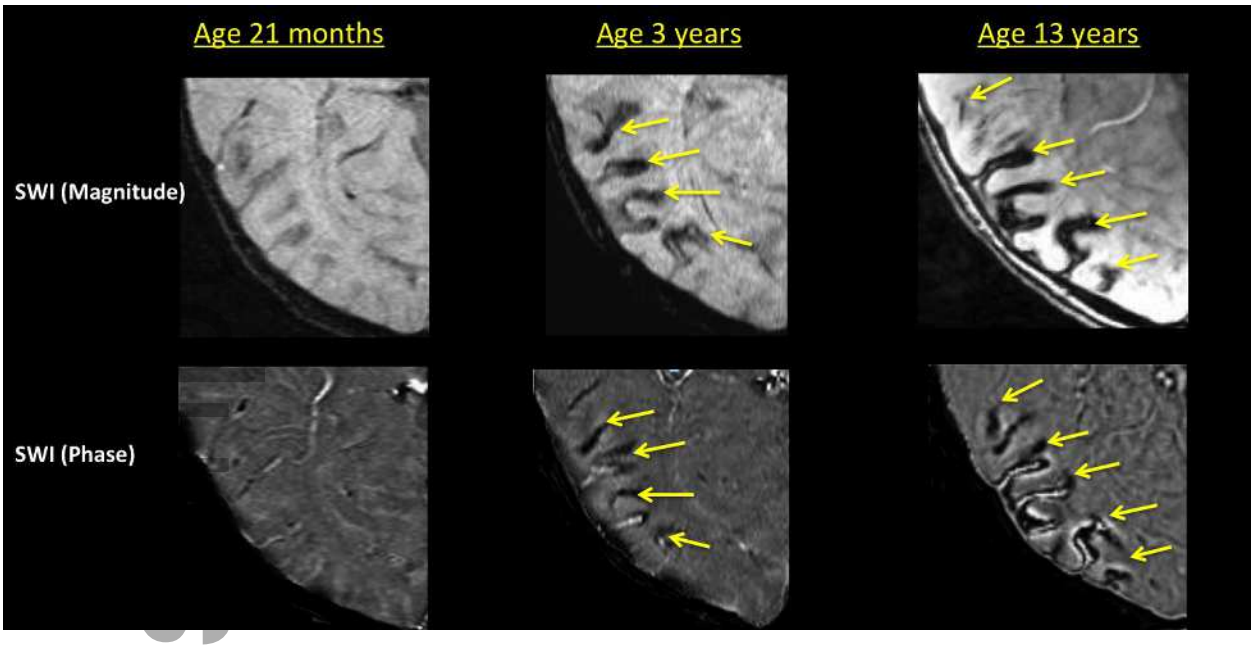

dmcn_13433_f2.jpg

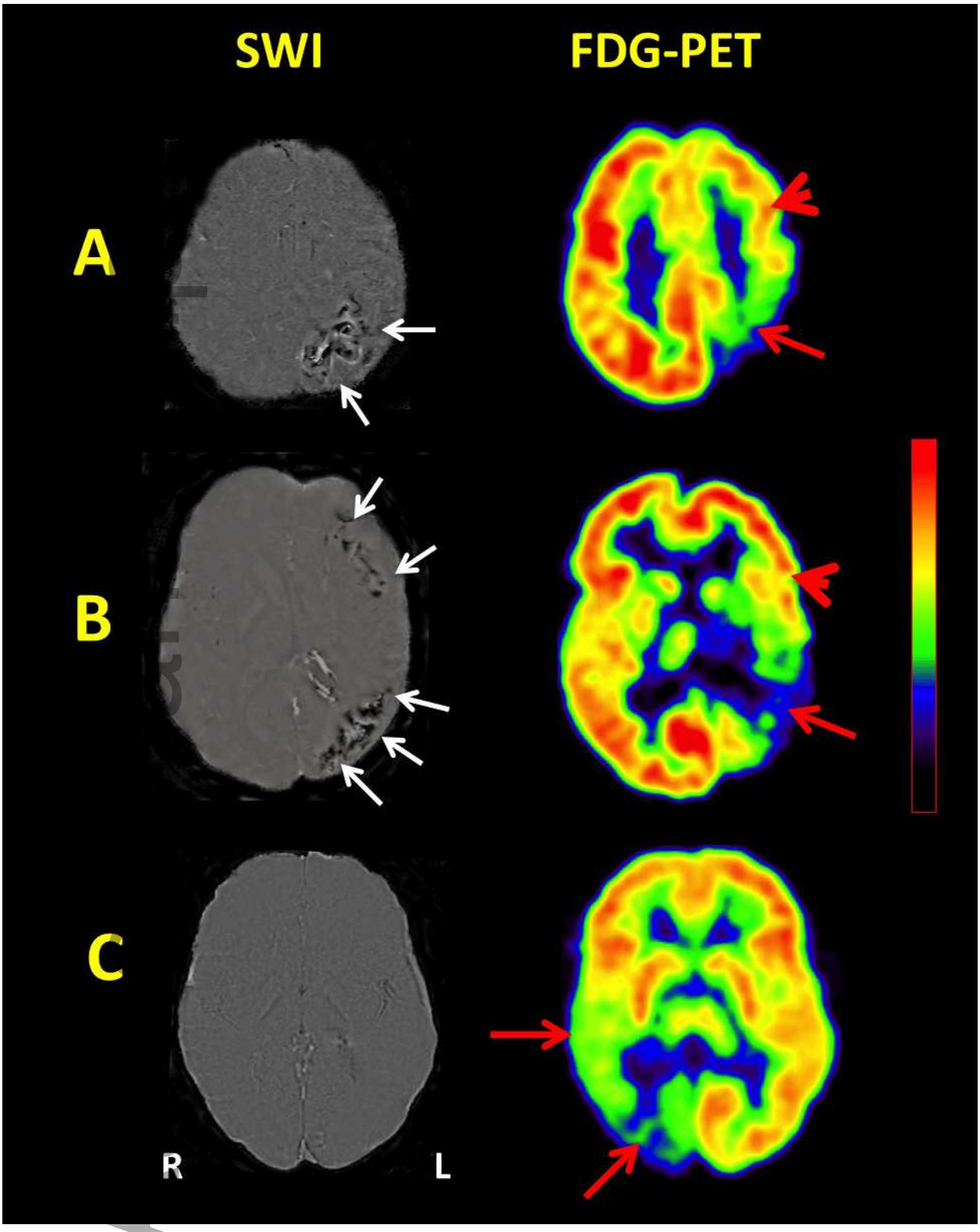

dmcn_13433_f3.jpg